Review of Scientific Instruments

Development of an alkali chloride vapour-generating apparatus for calibration of ultraviolet absorption measurements

Cite as: Rev. Sci. Instrum. **88**, 023112 (2017); https://doi.org/10.1063/1.4975590
Submitted: 30 September 2016 • Accepted: 22 January 2017 • Published Online: 16 February 2017

T. Leffler, C. Brackmann, M. Berg, et al.

Development of an alkali chloride vapour-generating apparatus for calibration of ultraviolet absorption measurements

T. Leffler,[1,2,a)] C. Brackmann,[2] M. Berg,[1] M. Aldén,[2] and Z. S. Li[2]
[1]*R&D, Strategic Development, Vattenfall AB, 814 26 Älvkarleby, Sweden*
[2]*Division of Combustion Physics, Lund University, Box 118, SE-221 00 Lund, Sweden*

(Received 30 September 2016; accepted 22 January 2017; published online 16 February 2017)

A novel design of alkali chloride vapour-generating cell has been developed, which can serve as a calibration cell for quantitative ultraviolet absorption concentration measurements and meticulous spectral investigations of alkali compounds. The calibration cell was designed to provide alkali vapour of well-controlled concentrations and temperatures, and consisted of a sealed quartz cell measuring 0.4 m in length with a temperature-controlled reservoir containing solid alkali salt. The cell was placed in a furnace and the alkali vapours generated from the reservoir have direct access to the measuring chamber. Investigations of potassium chloride (KCl) were made on sublimated vapour at temperatures 650, 700, 750, 780, and 800 °C while the reservoir temperature was kept 50 °C lower to avoid condensation. The cell provides stable KCl vapour pressures, and the furnace provides a homogenous temperature profile along the cell. KCl vapour pressures are well characterised and conform the base for determination of the KCl concentration in the cell. The alkali chloride levels matched the concentration range of the absorption setup and indicated a previously employed calibration method to overestimate KCl concentrations. The KCl absorption cross sections for wavelengths $\lambda = 197.6$ nm and $\lambda = 246.2$ nm were calculated to be 3.4×10^{-17} and 2.9×10^{-17} cm^2/molecule, respectively. The absorption cross section spectra did not show any structural differences with increasing temperature, which could indicate influence of dimers or significant changes of the population in the KCl vibrational states. The KCl absorption cross sections thus did not show any temperature dependence in the temperature region of 700–800 °C. Moreover, the applicability of the calibration cell for measurement of other alkali chlorides and hydroxides is discussed. [http://dx.doi.org/10.1063/1.4975590]

I. INTRODUCTION

Formation of harmful corrosive alkali compounds during combustion makes measurements of alkali chlorides or hydroxides in the flue gas of biomass-fired boilers of strong interest. Such measurements are relevant for fuel-quality assessments in terms of alkali-chloride formation,[1] operating conditions adjustments, and also the monitoring of the effects of alkali chloride reduction concepts, e.g., by addition of suitable additives.[2,3] Measurements can be performed with different optical or spectroscopic techniques and Monkhouse[4] has made a thorough review of online measurements using such methods on alkali metal species. While quantitative species concentrations in principle can be achieved by evaluation of measurements using the literature data for necessary physical quantities, e.g., absorption cross sections, for many cases, calibration under well-defined experimental conditions is necessary. For example, there might be insufficient data for relevant species such as an absorption cross section for potassium hydroxide as reported by Sorvajärvi *et al.*[5] New techniques developed for flue gas measurements, such as the LIDAR concept for KCl detection,[6] also require calibration for accurate quantitative measurements. Moreover, extension of instruments based on broadband absorption such as the *in situ* alkali chloride monitor (IACM)[7,8] to incorporate additional alkali species also call for the possibility to measure well-defined reference spectra. There is thus a demand for development of a suitable calibration cell to produce spectra of different alkali compounds under well-controlled conditions that can subsequently be used to carry out reliable quantitative determination of concentrations. This type of calibration cell also facilitates the possibility to carry out detailed spectroscopic studies of how the absorption cross section of different alkali compounds varies with temperature and due to formation of dimers.

Three different designs of high-temperature calibration cells for alkali compounds at atmospheric (open cell) and lower pressures (sealed cell) from the literature have been studied and are briefly described below. Grosch *et al.*[9] have developed a high-temperature open flow cell for reactive gases at temperatures up to 530 °C. This flow cell allows for high-resolution spectroscopic measurements in the ultraviolet (UV) and infrared (IR) spectral regions (190–20 000 nm). Vattenfall Research and Development AB has developed and patented an *in situ* alkali chloride monitor (IACM)[7] based on UV absorption and designed a calibration cell[8] for this instrument. This calibration cell operates at atmospheric pressure where solid

a)Electronic mail: tomas.leffler@forbrf.lth.se

potassium chloride is vaporized at 781 °C and the KCl vapour is subsequently diluted with N_2 and transported to a measuring chamber. The diluted KCl vapour is super-heated to 860 °C on its way to the measuring chamber where the concentration is evaluated. Davidovits and Brodhead[10] report on a sealed evacuated cell made of quartz with a diameter of 20 mm and a length of 20 mm where a sealed-off tip functions as a salt reservoir. The cell is placed in a furnace with additional heaters for the cell windows and the temperature of the salt reservoir is controlled by a conduction cooling rod. To avoid condensation, the salt reservoir is kept at a temperature of about 10 °C lower than that of the cell. Measurements were carried out on alkali halide vapours where investigations of potassium chloride and sodium chloride vapours are relevant for comparison with this work.[10]

Nevertheless, there is need for a calibration cell that generates vapours from alkali compounds at stable, well-defined concentration levels, and allows for optical measurements at well-controlled temperatures, which has motivated this research. The working hypothesis of this study is to verify that the new design of the calibration cell is fit for this purpose.

A novel calibration cell, which is based on a cold-finger arrangement and offers the possibility to generate sublimated vapour of KCl or other alkali compounds, is presented in this paper. Vapour is generated from a solid sample located in a small reservoir and the vapour pressure, controlled by the reservoir temperature, determines the concentration of the compound in the cell. The KCl vapour pressure in the cell can in turn be monitored at different pre-defined temperatures.

The outcome of this study is convincing and the design can be used for investigations of other solid chemical components, which are of relevance for, in this particular case, biomass and waste combustion. The calibration cell presented in this paper is stable and robust, which facilitates handling and experimental reproducibility, which in turn result in accurate and reliable calibration data.

II. EXPERIMENTAL

A. The calibration cell

The calibration cell, schematically shown in Figure 1(a), was made of a quartz tube with outer and inner diameters of 30 and 27 mm, respectively. Windows made of quartz (SILUX®3) were fused onto each end of the tube at an angle of 45°. The optical path length at the centre line of the cell is 400 mm and a salt reservoir, containing around 2 g of crystalline KCl (EMSURE®, 1.04936.0500), was placed at the centre part of the cell. Before sealing the cell, the pressure inside the cell was brought down to vacuum (1.33×10^{-4} Pa) and it was then filled with argon to a pressure of 100 Pa at room temperature. Precise control of the KCl salt temperature is crucial for the performance of the calibration cell and a special design is adopted in this work. In order to achieve precise and independent control of the temperature of the salt reservoir enclosed in the calibration cell, two quartz tubes were fused together to build up a double-jacketed tube structure for cooling. The cooling tube was subsequently fused together with the cell in such a way that the salt reservoir ended up in the centre of the cooling tube (cf. Figure 1(a)). This permits keeping the salt at a controlled temperature during the experiments by regulating a suitable flow of N_2 through the cooling tube.

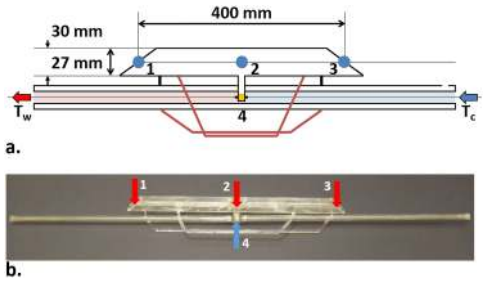

FIG. 1. (a) Detailed schematic of the calibration cell. (b) Photo of the calibration cell with the locations of the thermocouples mounted on the cell indicated. Numbers 1-3 indicate positions of pairs of thermocouples for measurement and control of cell temperature. Number 4 indicates the position of the salt reservoir and the two thermocouples attached to it.

Before the cell was placed into the furnace, eight thermocouples (type K) and a Swagelok connector for the cooling gas were mounted onto the cell. Six thermocouples were mounted along the side of the cell with two in the centre (position 2, Figures 1(a) and 1(b)) and two at each end (positions 1, 3, Figures 1(a) and 1(b)). Three of these thermocouples were used to monitor the cell temperature, while the remaining three were used by the temperature regulators to control the temperature in the furnace and consequently the cell temperature. Two thermocouples (position 4, Figures 1(a) and 1(b)) were used to measure the salt (KCl) reservoir temperature, one (T_c) was mounted together with the Swagelok connector (not shown in Figure 1(b)) that supplies the cooling gas to the cell, while the other (T_w) was inserted into the cooling tube from the opposite side.

The thermocouples used to measure cell temperature were connected to a logger system together with the thermocouples connected to the cold (T_c) and warm (T_w) sides of the salt reservoir. The cold side of the salt reservoir is the wind side (to the right side of the salt reservoir shown in Figure 1(a)) and the warm side is the lee side (to the left side of the salt reservoir shown in Figure 1(a)). The logger system included a standard computer connected to a Hydra Data Acquisition Unit 2620A (Fluke). The calibration cell was equipped with supporting legs to keep its position in the furnace stable, as shown in Figure 1 and in Figure 2(b) presenting the calibration cell in the furnace.

B. The furnace

Figure 2(a) shows a schematic of the furnace with its temperature-controlling device, absorption setup, and calibration cell. Figure 2(b) shows a photo of the calibration cell when it is placed in the furnace. The furnace was constructed as follows: three pieces of Kanthal D wire with an equal length of 15 m and a diameter of 1 mm were cut from a cable reel. The resistivity of the wire was 1.733 Ω/m, which gave a total resistance of 26 Ω in each piece and subsequently a total power of 6 kW (3 × 2 kW) for the furnace at an applied voltage of 230 V. The electrical wires were manually wound one by one around a steel rod to form a spring-like heating element. A

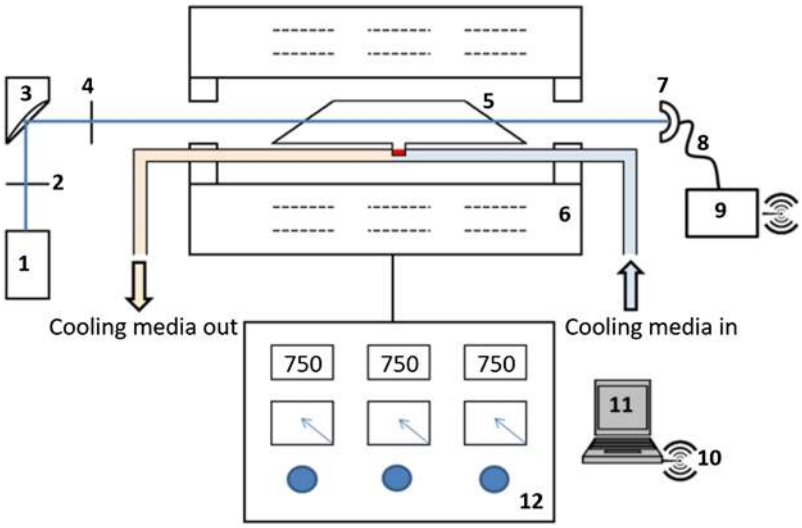

a.

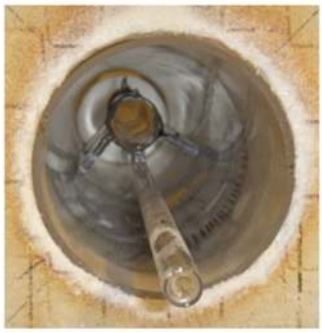

b.

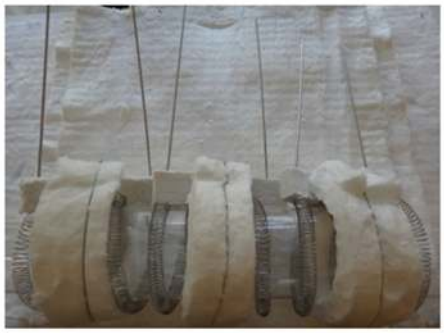

c.

FIG. 2. (a) Schematic of furnace, temperature control, calibration cell, and equipment for UV absorption spectroscopy. 1. UV light source; 2. aperture; 3. parabolic mirror; 4. aperture; 5. calibration cell; 6. furnace; 7. detection collimator; 8. optical fibre; 9. spectrometer; 10. Bluetooth connection between the spectrometer and the computer; 11. standard computer; 12. furnace temperature control unit. (b) Photo showing the calibration cells location in the furnace. (c) Photo showing the heating elements wound around the quartz tube forming the furnace chamber also seen in (b).

stainless steel pipe was connected at the wire ends of each heating element to provide a low-ohmic connection between the heating wire and the wire from the power supply. The heating elements were evenly distributed around a 670 mm long quartz tube with an internal diameter of 100 mm to create three individually controlled heating zones (photo in Figure 2(c)). The quartz tube with the heating elements was insulated with a 10 cm thick layer of durablanket (Fiberfrax) and then placed in a box built of 5 cm thick building blocks of duraboard (Fiberfrax). The temperature-controlling device for the furnace was built up with the following components: a three-phase residual-current device, three fuses, a safety switch, three solid-state relays, three power controllers, three Proportional-Integral-Derivative (PID) temperature controllers, and three current indicators. The power controllers were included to enable individual adjustment of the current to each heating element. The temperature limits of the glass material in the furnace and calibration cell, as given by the manufacturer (Scientific Lab Glass in Lund, Sweden), are 1150 °C for continuous operation and 1300 °C for experiments during shorter times.

C. The absorption spectroscopy setup

Absorption measurements on KCl vapour generated in the calibration cell were performed using an amended version of the IACM instrument[7] arranged in the experimental setup shown in Figure 2(a). The amendments consist of the following changes: the previously used xenon lamp has been replaced by a deuterium lamp; a lens and a spherical mirror have been replaced by two parabolic mirrors, where one of the parabolic mirrors (the collimator) is equipped with a SubMiniature version A (SMA) connector for the optical fibre.

UV light from the high-intensity deuterium lamp (1) (L1314, Hamamatsu) was radiated through an aperture (2) and collimated by a 2-in., 90° off-axis parabolic mirror (3) with UV-enhanced aluminium coating and a reflective focal length of 6 in. (Thorlabs). The collimated UV light beam subsequently passed through another aperture (4) and through the quartz windows on each side of the calibration cell (5), which in turn was located in the furnace (6). The transmitted light was collected in an UV-enhanced aluminium reflective collimator (7) with a diameter of 12 mm and an SMA connector for an optical fibre (Thorlabs). The collected UV light was then transferred through the optical fibre (8) (FC-UV600-0.5-SR, Azpect Photonics) and subsequently dispersed in a spectrometer (9) (AVABENCH-75-2048, Azpect Photonics) with an entrance slit of 50 μm width and a grating with 2400 grooves/mm. A Bluetooth device (10) (WCS-232, SystemBase) was used to transfer the data from the spectrometer to the computer. The collected spectrum was evaluated in a standard computer (11) by means of the differential optical absorption spectroscopy

(DOAS) technique[11] to retrieve the KCl concentration in the calibration cell.

D. The calibration of the thermocouples

Prior to the absorption measurements on KCl vapour the thermocouples were calibrated together against a reference thermocouple, which in turn had been calibrated according to EA-4/02 standard at a certified laboratory (Pentronic AB). The calculated expanded uncertainty for all calibrated temperatures was determined to be ±0.7 °C. The experimental system was calibrated for five temperatures: 600, 650, 700, 730, and 750 °C. The calibration started at temperature 750 °C which was progressively lowered down to 600 °C before the calibration process ended. Each temperature was stabilized during a time span of 2 h before the reference thermocouple was compared with the other thermocouples in the system.

E. Preparation and performance of the experiment

1. Placement of the cell into the furnace

The cell was placed in a central position in the furnace (cf. Figure 2(b)) and the hose that supplied the cooling medium was connected. Two insulating end plugs, each with a hole for the UV-beam to pass through the furnace and the cell, were placed at the ends of the furnace to minimize heat losses. The optical measurement system consisting of the UV-light source, optical components, and spectrometer was then placed at the respective end of the furnace and as a final step the UV-light beam was aligned through the cell.

2. Execution of the measurements

Five different saturated vapour pressures of KCl were generated by keeping the salt reservoir at temperatures 600, 650, 700, 730, and 750 °C. The trials were randomized to avoid any systematic errors. A measurement was performed in the following steps:

- The experiment was started by setting the selected temperature on each furnace temperature controller. Once the cell temperature had reached the set point value, it was kept there for approximately 1 h for temperature stabilization while the temperature on the salt reservoir was kept at 300 °C by regulating the cooling gas flow.
- A reference and a background spectrum was collected after 1 h and uploaded into the evaluation software; thereafter, the UV absorption measurements by means of the IACM instrument were made continuously during a time period of about 2 h with spectra measured every 10 s.
- The temperature of the salt reservoir was adjusted by the flow of the cooling medium to the selected temperature and was kept there for 2 h to allow the vapour pressure of the KCl inside the cell to reach thermodynamic equilibrium.
- The temperature of the salt reservoir was brought down to 300 °C by cooling with compressed air. Once the KCl concentration had reached 0 ppm, at 300 °C the experiment was considered completed and a new set point was added to the temperature controllers.

F. Determination of the KCl vapour pressure

The partial pressures of the KCl monomer and the K_2Cl_2 dimer in the calibration cell have been determined from the literature data on vapour pressures measured at different temperatures.[12] These data have been used to fit coefficients A, B, and C in the Antoine equation[13]

$$\ln p = A - \frac{B}{C+T}. \tag{2.1}$$

The coefficients were fitted in Excel using the LINEST function and Eq. (2.1) allows to calculate the vapour pressure at different temperatures, where p (Pa) represents the vapour pressure and T (K) the temperature. The coefficients for KCl were determined as $A = 11.35$, $B = 3659.18$, and $C = -581.64$.

The same procedure was used to determine the Antoine coefficients A, B, and C for K_2Cl_2 vapour pressures using data at corresponding temperatures from the literature.[12] The coefficients for K_2Cl_2 were determined as $A = 10.96$, $B = 3874.74$, and $C = -600.21$.

Vapour pressures thus calculated by Eq. (2.1) have also been compared with vapour pressures calculated with the commercial HSC Chemistry 7.1 software[14] based on extensive compilation of thermochemical data therein.[15–26]

In addition, the vapour pressure was calculated utilizing the Clausius-Clapeyron equation

$$p_2 = p_1 exp\left(-\frac{\Delta H_{sub}}{R}\left(\frac{1}{T_2} - \frac{1}{T_1}\right)\right). \tag{2.2}$$

The Clausius-Clapeyron equation is an approximation where it has been assumed that the vapour volume is much larger than the solid volume, that the sublimation enthalpy ΔH_{sub} is constant in the measurement region and finally that the KCl vapour behaves as an ideal gas.[13] In Equation (2.2), R is the universal gas constant, p_1 and T_1 are the pressure and temperature at state 1, T_2 is the temperature at state 2, and p_2 is the calculated vapour pressure at state 2. In the input data for state 1, $T_1 = 900$ K, the vapour pressure $p_1 = 1.04$ Pa has been calculated by Equation (3) presented by Mayer and Wintner,[27] and the sublimation enthalpy $\Delta H_{sub} = 211\,716$ J/mol has been calculated with Equation (4).[27] The values of the constants used in the mentioned equations have been retrieved from Table IV in the same reference.[27]

G. KCl spectral simulations

The vibrational and rotational energy level structure of the KCl ground state was calculated using the PGOPHER[28] software with molecular constants obtained from Barton *et al.*[29] Spectral simulations at different temperatures provided energy level population fractions and allowed for analysis of population redistributions between vibrational levels.

III. RESULTS AND DISCUSSION

Figure 3 presents salt reservoir temperature, kept at 730 °C, and the calculated KCl vapour pressure in the calibration cell, which was maintained at a temperature of 780 °C,

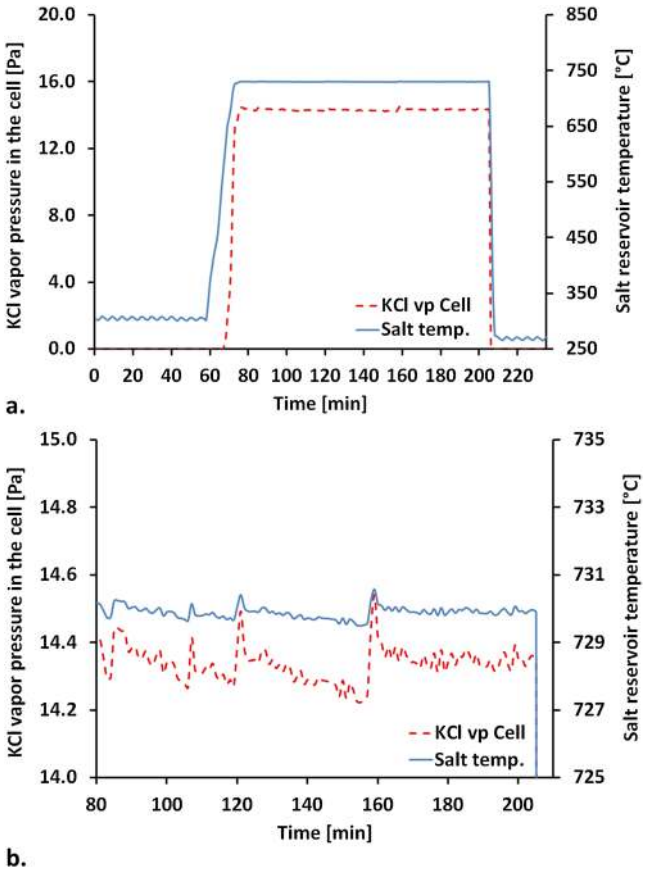

FIG. 3. (a) Salt reservoir temperature (solid line) measured in the calibration cell and its corresponding KCl vapour pressure (dashed line) at 730/780 °C. (b) Close-up plot added to clearly show small variations in temperature and their impact on KCl vapour pressure in the cell during the measurement. The temperature was measured and corresponding vapour pressures were calculated every minute.

versus time during the experiment. Hereafter, the used calibration cell temperatures will be presented as salt reservoir temperature/cell temperature (730/780 °C).

The salt reservoir temperature between minutes 90 and 200 (cf. Figure 3(a)) is rather stable at 730 °C, except for three minor adjustments of less than 1 °C, cf. Figure 3(b). These three adjustments were made at minutes 105, 120, and 160. The average salt temperature during the experiment was 729.9 °C with a standard deviation of 0.17 °C and maximum and minimum temperatures of 730.4 and 729.6 °C, respectively. The three salt temperature corrections also affected the KCl vapour pressure in the cell, as shown in Figure 3(a) and more in detail in Figure 3(b). The KCl vapour pressure calculated in the cell during the experiment was on average 14.3 Pa with a standard deviation of 0.05 Pa and maximum and minimum vapour pressures of 14.5 and 14.2 Pa, respectively. The oscillations in the salt temperature before (minutes 0–60) and after (minutes 205–230) the experiment were due to temperature or flow changes in the compressed air used as a cooling medium on these occasions. These oscillations were avoided during the experiment by switching from compressed air to N_2. However, the salt reservoir temperature and subsequently the KCl vapour pressure in the calibration cell could be even better stabilized with an automatic temperature controller instead of manual control (adjusting a needle valve), as was the case for this experiment. This was verified during the last 30 min (minutes 175–205) of the experiment when very stable operation was achieved (cf. Figure 3(b)). During minutes 175–205, the average salt temperature was 729.9 °C with a standard deviation of 0.07 °C and the difference between the maximum and minimum temperature was 0.3 °C. The average KCl vapour pressure during the same time span was 14.3 Pa with a standard deviation of 0.02 Pa, i.e., on the order of 0.14%, and a difference between a maximum and minimum concentration of 0.1 Pa. Thus, the cell is able to maintain very stable KCl concentration levels at desired temperature.

Figure 4 shows the temperature measured at three locations on the cell: the left end, the middle, and the right end when the temperature in the cell was set to 780 °C. Initially, with sufficient cooling flow to maintain the reservoir temperature at 300 °C, the temperatures in Figure 4 follow values set by the temperature controllers of the furnace. The experiment started after around 60 min when the cooling flow was reduced and switched to N_2 to obtain a stable reservoir temperature of 730 °C, sufficient for generation of detectable vapour but still 50 °C lower than the cell to avoid condensation in the measuring chamber. At this time, the temperature at the right end (line with dots) and in the middle (line with diamonds) started to decrease and increase, respectively (cf. Figure 4). This is presumably due to two separate reasons. Firstly, the thermocouples mounted on the cell might be too close to the tube that cools the salt reservoir since the tube is not provided with any radiation shield (cf. Figure 1(b)). This might change the temperature profile in the vicinity of the thermocouples, which control the temperature in the furnace. Radiation from the heating elements of the furnace in combination with reduced losses from the cooling tube is believed to be the cause for the temperature drop in the right part of the calibration cell at minutes 60 (cf. Figure 4). Secondly, it seems probable that the heating zones in the furnace are close enough to influence each other. During experiments it has been observed that the middle temperature controller of the furnace has not been able to follow the set point. The middle temperature has been around 10 °C too high in each experiment, as can be observed in the corresponding profile at minutes 60 in

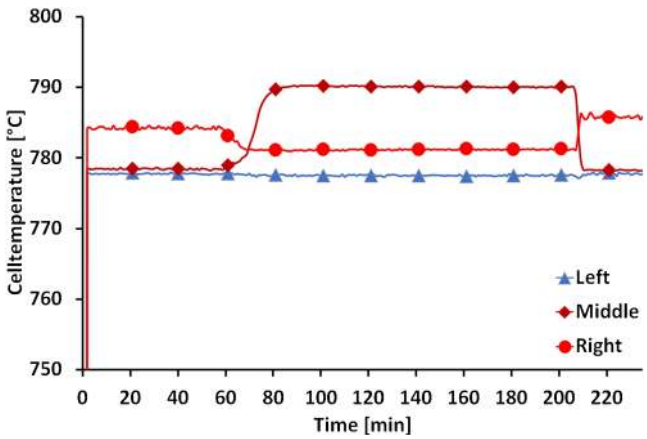

FIG. 4. Temperature on the left side of the cell (line with triangles), in the middle (line with diamonds), and at the right side (line with dots) in the calibration cell during the experiment.

Figure 4, and is probably due to heating from the surrounding zones.

However, the slight temperature difference of 12 °C between the middle point and the ends is acceptable. This corresponds to a relative difference in absolute temperature on the order of 1% and a corresponding change in gas density and absorbance in the cell. Thus, the cell temperature is sufficiently homogenous for calibration measurements under well-defined conditions.

Reference spectra were sampled when the salt reservoir was kept at low temperature (about 300 °C) and no absorption was expected. The reference spectrum (rf) in Figure 5(a) is an average of such spectra sampled at cell temperatures 650, 700, 750, 780, and 800 °C. The measured spectra (ms) shown in Figure 5(a) were sampled when the salt reservoir temperature was kept at 600 (599.1), 650 (650.0), 700 (700.1), 730 (729.9), and 750 (749.6) °C, i.e., 50 °C below the corresponding cell temperature, resulting in sufficient vapour in the cell for absorption.

The absorbance spectra of KCl in Figure 5(b), obtained for different salt temperatures, have been evaluated in the following way: firstly, a normalized spectrum is obtained by calculating the measured spectrum minus the background spectrum divided by the reference spectrum minus the background spectrum. Secondly, the negative natural logarithm of the resulting spectrum is calculated. The noise appearing in the raw data shown in Figure 5(a) is mostly caused by the uneven response of the pixels in the CCD detector of the spectrometer. The noise disappears once the measured and reference spectra have been divided with each other, as per the absorbance spectra in Figure 5(b). It is shown in Figure 5(b) that gas-phase KCl has two major absorption regions: region 1, 200–220 nm and region 2, 230–300 nm as discussed by Davidovits and Brodhead.[10] The absorbance in region 2 at temperatures 650 °C and 800 °C corresponds to ~5% and 85% absorption of light through the cell, respectively, and the KCl concentration is evaluated in this region by means of differential optical absorption spectroscopy (DOAS).[11] The absorption measurements performed with this setup at a cell temperature of 650 °C with the corresponding salt reservoir temperature at 599.8 °C results in a maximum absorbance of 0.04 and sets the lower detection limit for this measurement system (cf. Figure 5(b)).

The vapour pressures in the calibration cell and subsequently the KCl concentration are based on 38 vapour pressure data points in the temperature region of 576–766 °C obtained from the literature.[12] The Antoine equation (2.1) with its coefficients was derived from the literature data and used to calculate the vapour pressure of KCl at reservoir temperatures: 600 (599.8), 650, 700 (700.2), 730 (729.9), and 750 (749.6) °C. For comparison, vapour pressure calculations were also made with the Clausius-Clapeyron equation and the HSC Chemistry 7.1 software.[14] The results from these calculations are presented in Figure 6 together with the experimental raw data[12] used to fit the Antoine equation coefficients.

Figure 6 shows that all calculations and the original experimental data of van der Kemp[12] agree well with each other up to temperature 640 °C. At around 660 °C, the values obtained from the Clausius-Clapeyron equation start to deviate and appear higher than those of the other calculations. Since the Clausius-Clapeyron equation is an approximation it is reasonable that its values deviate from the rest. When

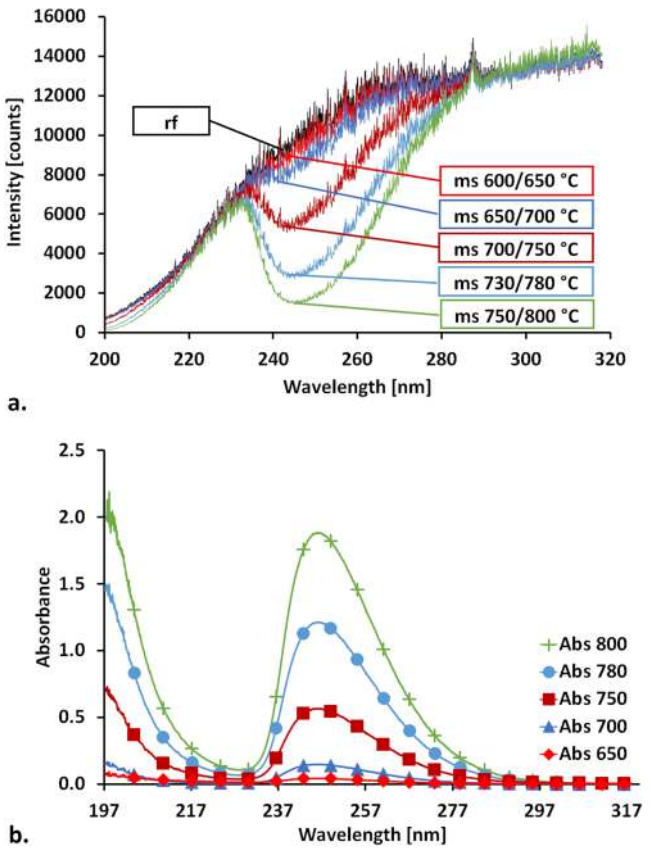

FIG. 5. (a) Reference and measured spectra at cell temperatures 600/650, 650/700, 700/750, 730/780, and 750/800 °C (rf = reference spectrum and ms = measured spectrum, numbers behind ms indicate the salt reservoir and cell temperature). Each spectrum is an average of 200 sampled spectra. (b) Absorbance spectra for cell temperatures 650 (line with diamonds), 700 (line with triangles), 750 (line with squares), 780 (line with dots), and 800 (line with crosses) °C. The symbols have been inserted to help spectrum identification in the plot.

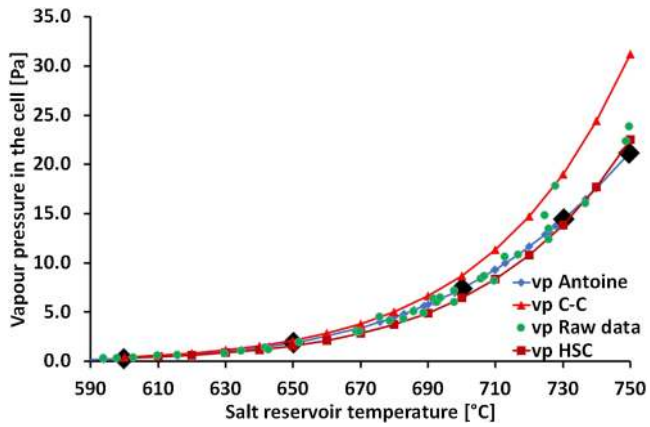

FIG. 6. KCl vapour pressure calculated by the Clausius-Clapeyron equation (vp C-C, triangles), calculated by the Antoine equation determined by the literature data (vp Antoine, diamonds), of the raw data used to determine the Antione coefficients (vp Raw data, dots), and calculated by the HSC software (vp HSC, squares). Vapour pressures determined using the Antoine equation for temperatures of the performed experiments are marked with black larger diamonds.

the temperature reaches around 700 °C it can be seen that the experimental data (dots) start to fluctuate more than previously. However, with the exception of the two highest vapour pressure measurements from van der Kemp[12] at 730 °C, it can be seen that the calculations by the Antoine equation and the HSC software follow the experimental data. Thus, KCl vapour pressures in the investigated temperature regime are well characterized.

Nevertheless, thorough vapour pressure measurements in the temperature region of 700–750 °C could improve the accuracy of the experimental data further. That would lead to increased accuracy and reliability for the calculated vapour pressure and subsequently the determined KCl concentration in the cell. In the following, the Antoine equation, based on experimental data, has been used to calculate the vapour pressures in the cell for the reservoir temperatures of the performed measurements. These vapour pressure values are indicated by larger black diamond symbols in Figure 6. From Figure 5(b) it can be seen that the absorbance measured for cell temperature 600/650 °C indicates the detection limit for the present experimental configuration. From Figure 6 it can be seen that this corresponds to a vapour pressure of less than 1 (0.3) Pa. Improved sensitivity could be achieved using multiple passages through the cell to increase the absorption path length.

Calculated KCl vapour pressures in the cell at the investigated reservoir temperatures are shown with the diamond symbols in Figure 7. The uncertainty in the salt reservoir temperature directly affects the accuracy of the calculated KCl vapour pressure in the calibration cell and thermocouple calibrations indicate an uncertainty in measured temperatures of 5 °C. In addition, a possible positive temperature offset of 15 °C, caused by the movement of the thermocouple that measured the salt reservoir temperature, was identified. During a set of measurements, it was found that the thermocouple had moved away from the salt reservoir, possibly due to thermal expansion in the thermocouple originating from the randomized trials where the salt reservoir experiences temperature changes between 300 and 450 °C. These temperature changes occur at the beginning of an experiment (increasing the salt reservoir temperature) and at the end of an experiment (decreasing the salt reservoir temperature). The problem was solved by inserting a thin metal wire in the cooling tube from the opposite side to that of the thermocouple and connect it to the thermocouple. This made it possible to pull the thermocouple back and place it in position before a new experiment was started. On a few occasions it was observed that the reservoir temperature reading dropped about 10–15 °C when the thermocouple was pulled back by means of the metal wire. Thus, such shift in thermocouple position could potentially mean that the reading provides an overestimation of the reservoir temperature and vapour pressure. A correct salt reservoir temperature results in a correctly determined vapour pressure, which is subsequently used to produce a calibration spectrum. An overestimated salt reservoir temperature due to the offset in thermocouple position as outlined above results in an overdetermined vapour pressure. The combined effects of thermocouple uncertainties and the temperature offset were investigated in evaluations assuming a salt reservoir temperature 15 °C lower and 5 °C higher than the thermocouple reading. The results are indicated by the error bars in Figure 7 showing KCl vapour pressures to be either over predicted by 23%–49% or under predicted by 8%–23% with the largest relative errors obtained for the lowest temperature.

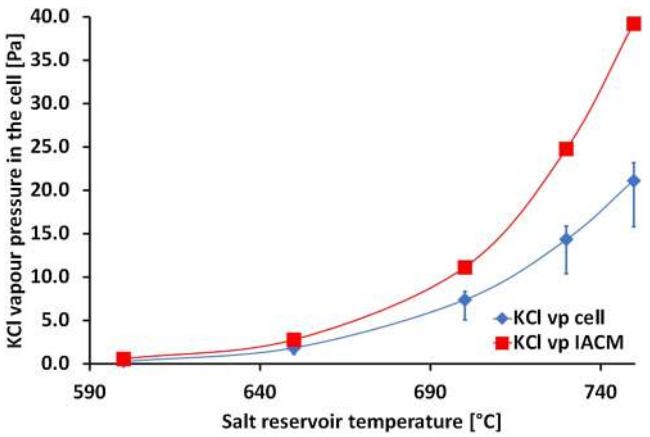

FIG. 7. KCl vapour pressure from all experiments, obtained by IACM (KCl vp IACM, line with squares), and calculated by the Antoine equation, Eq. (2.1) (KCl vp cell, line with diamonds). Each measurement point has been assigned its proper error bar. The error bars for KCl vp IACM are so small that they are covered by their symbol. Details are given in the main text.

The IACM instrument has been used to measure KCl concentrations, which have been recalculated to vapour pressures in the calibration cell and the results are shown as square symbols in Figure 7. The measured KCl vapour pressures are about 75%–100% higher than those determined from calculations with the largest error referring to the lowest temperature/vapour pressure. The differences are significantly higher than the uncertainties estimated for the cell vapour pressures as described above and are probably related to the original calibration procedure on which the absorption evaluation is based.[8] In the evaluation, the measured spectrum is fitted to a calibration spectrum measured during continuous evaporation of a certain mass of KCl transported through a calibration cell placed in a furnace.[8] Possible sources of error are salt losses during transport to the cell, a non-uniform temperature profile in the furnace, and pressure build-up in the calibration cell. During operation of this previous calibration equipment it has been noticed that absorption spectra on occasion show traces of previously measured compounds, which indicates that salt vapour can stick to the walls of the tube, which transports a gas-mixture of N_2 and vaporized KCl to the measuring chamber. A temperature gradient in the calibration cell will result in a density gradient of KCl molecules, which introduces a bias in absorption towards low-temperature high-density regions. Even though the calibration cell is built of aluminium oxide, the KCl vapour might induce corrosion in the surrounding steel tubes. Corrosion products could potentially lead to a pressure increase in the cell, which is assumed to have atmospheric pressure during normal conditions, resulting in an excessively high absorption spectrum and in turn a too low concentration value for the calibration spectrum.

Uncertainties due to salt losses, non-uniform temperature profile, and pressure build-up in the previous calibration

cell have been considered for and are avoided in the newly developed calibration cell presented in this article. Salt losses are avoided in the sealed cell and the salt reservoir has been made the coldest point of the cell, which determines the vapour pressure. Any wall effects, which result in a pressure drop, will automatically be corrected by the vapour pressure set according to the salt reservoir temperature. In this design, pairs of thermocouples mounted on the cell at the ends and in the middle for combined control and measurements of the temperature ensure that inhomogeneities in cell temperature and accordingly vapour number densities are minimized, which then renders a reliable absorption spectrum. The only pressure build-up in the calibration cell originates from argon, increased from 100 Pa at room temperature, and the pressure of KCl and K_2Cl_2 vapours at the cell temperature. This avoids unknown pressure build-ups. The new calibration cell has been operated at salt reservoir temperatures of 600, 650, 700, 730, and 750 °C and repeated measurements in randomized orders give reproducible calibration spectra evaluated to the same vapour pressures.

A factor for consideration when comparing calculated and measured KCl vapour pressures in the cell is the formation of the dimer K_2Cl_2. For the investigated temperatures, the vapour pressure of this compound is around 20% of that of KCl[12] and the dimer contribution to the total pressure is small. The dimer possibly contributes to the UV absorption spectra as suggested by Davidovits and Brodhead.[10] However, this could likely not explain the overestimation of KCl vapour pressures when evaluating the cell spectra using the IACM evaluation procedure since it is based on fit to a calibration spectrum measured on vaporized KCl, which also will contain dimer contributions.

Figure 8 shows KCl UV absorption cross sections evaluated from measurements at five different KCl vapour pressures generated at the following salt reservoir/cell temperatures: 600/650, 650/700, 700/750, 730/780, and 750/800 °C. With the exception of the profile obtained for measurement at temperatures 600/650 °C, for which the uncertainty in KCl vapour pressure is the largest and the absorption in the cell is lowest, the profiles are grouped fairly well together in spite of the large variation in vapour pressures. The absorption from the KCl ground state to the unbound excited state is dependent on the ground state energy level population determined by the temperature-dependent Boltzmann distribution. This would in turn introduce a temperature dependence of the absorption spectral profiles. The absorbance spectra in Fig. 9(a) were normalized to investigate if other temperature effects apart from changes in gas density could be observed as changes in spectral shape.

With the exception of the spectrum corresponding to temperature combination 600/650 °C, the spectra show similar shape and do not indicate any temperature effects.

Population fractions for vibrational levels of the KCl ground state calculated for the investigated cell temperatures are shown in Fig. 9(b). Vibrational levels of quantum number v = 0, 1, and 2 contain about 70% of the population and on the order of 6% of the population of these levels is redistributed to higher vibrational levels when the temperature is increased from 650 to 800 °C. This suggests a weak temperature dependence in agreement with the observed consistent shape of the normalized spectra for temperatures 650/700, 700/750, 730/780, and 750/800 °C in Fig. 9(a). The redistributed population for temperature changes between 650 and 700 °C is on the order of 2%. The prominent difference in absorption cross sections observed between temperatures 600/650 and 650/700 °C (cf. Fig. 8) is likely due to the previously discussed uncertainties in temperature and KCl vapour pressure at temperature 600/650 °C. For example, assuming an increased salt reservoir temperature of 10 °C would place the absorption

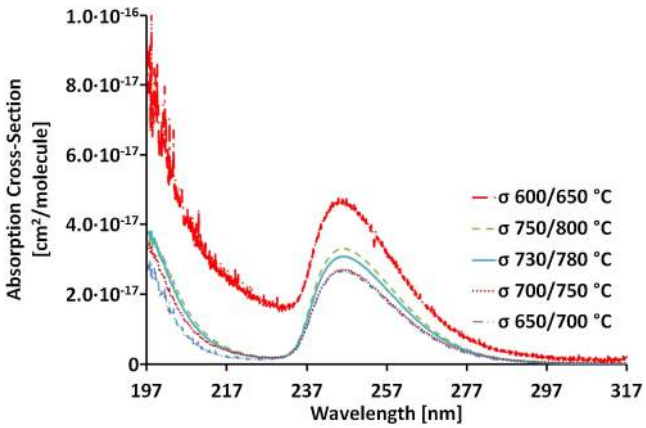

FIG. 8. UV absorption cross section for gas-phase potassium chloride at different temperatures.

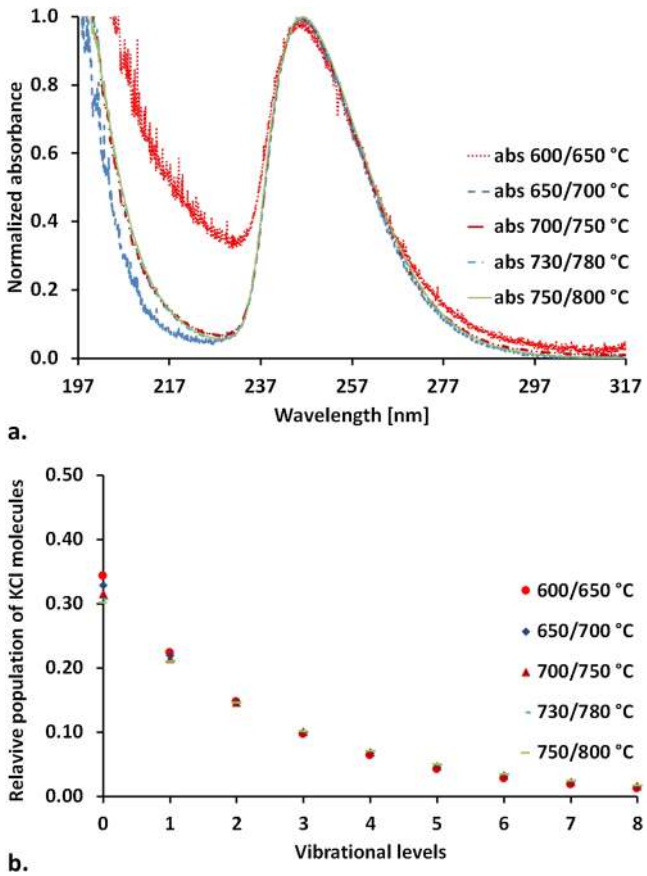

FIG. 9. (a) Normalized absorbance spectra and (b) the relative population of vibrational levels for potassium chloride at cell temperatures 600/650, 650/700, 700/750, 730/780, and 750/800 °C.

cross section for temperature of 600/650 °C with the other values.

Vapour pressures of the KCl monomer and the K_2Cl_2 dimer have different temperature dependencies and even though the monomer pressure remains higher at all temperatures, dimer formation is increasingly favoured at higher temperatures.[12] Significant contributions from both of these components to the absorption spectrum would therefore most likely introduce changes in spectral shape with temperature. The similarity in shape observed for the majority of the normalized absorbance spectra (cf. Fig. 9(a)) thus suggests that the monomer, dominant at lower temperatures, remains the main contribution to the absorbance spectrum.

Figure 10 shows the KCl absorption cross section versus cell temperature for the shortest wavelength of the measurement system, $\lambda = 197.6$ nm, and for the peak wavelength $\lambda = 246.2$ nm, both retrieved from the absorption spectra shown in Figure 8. As also indicated in Figure 9(a), the absorption cross sections for the cell temperature of 600/650 °C deviate considerably compared to the rest. This is believed to be due to large uncertainty in the vapour pressure, as discussed previously. Since the other four cross section values for wavelengths $\lambda = 197.6$ nm and $\lambda = 246.2$ nm, respectively, are scattered around horizontal lines, they indicate that the absorption cross sections are temperature-independent in the evaluated temperature region of 700–800 °C. The average absorption cross section for the two wavelengths has been calculated to be 3.4×10^{-17} cm^2/molecule with a standard deviation of 4.2×10^{-18} cm^2 for $\lambda = 197.6$ nm and 2.9×10^{-17} cm^2/molecule with a standard deviation of 3.0×10^{-18} cm^2 for $\lambda = 246.2$ nm.

Short wavelengths approaching the vacuum ultraviolet region below 200 nm can be employed for alkali compound detection by means of laser-based photofragmentation fluorescence, for example, using excimer lasers at $\lambda = 193$ nm.[30,31] Thus, KCl absorption cross sections in this wavelength region are of interest for quantitative analysis of laser induced photofragmentation data.

The absorption cross section at $\lambda = 246$ nm determined by Davidovits and Brodhead[10] on vapours of melted KCl in a temperature region of 841 to 951 °C was 2.0×10^{-17} cm^2/molecule. The average absorption cross section determined on sublimated vapour in the calibration cell at the same wavelength was calculated to be 2.9×10^{-17} cm^2/molecule in a temperature region of 700–800 °C. A comparison between the absorption cross sections shows the value of Davidovits and Brodhead to be about 70% of that determined in the calibration cell. The absorption cross section determined in the calibration cell for $\lambda = 197.6$ nm shows a slightly higher value than for $\lambda = 246.2$ nm, which is also reported by Davidovits and Brodhead.[10] Thus, also at shorter wavelengths below 200 nm, the values measured by Davidovits and Brodhead are lower than the values obtained in the calibration cell. However, Oldenborg and Baughcum[31] determined the absorption cross section of KCl to be $(4.1 \pm 0.6) \times 10^{-17}$ cm^2/molecule at $\lambda = 193.4$ nm, which is in good agreement with that determined in the calibration cell for $\lambda = 197.6$ nm.

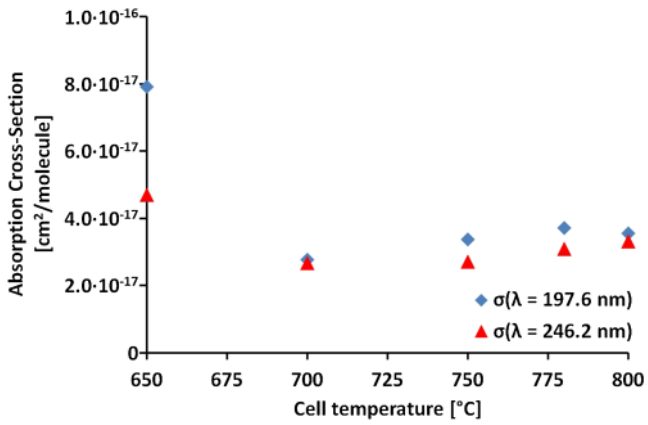

FIG. 10. Absorption cross sections of gas-phase potassium chloride at elevated temperatures for wavelengths $\lambda = 197.6$ nm and $\lambda = 246.2$ nm.

The cell presented in this article can easily be used to generate calibration spectra of other alkali compounds, such as sodium chloride (NaCl), which is of interest in waste and coal combustion. This compound has vapour pressures rather close to those of KCl and the cell could thus be operated under conditions similar to those for the investigations of KCl. There is also a need for calibration data for sodium hydroxide (NaOH) and for potassium hydroxide (KOH).[5] Previous studies indicate that hydroxides exhibit lower absorption cross sections than chlorides.[32] Moreover, since vapour pressures for solid-gas equilibrium for these compounds are rather low,[14] the cell needs to be operated above the melting points, 318 °C for NaOH and 406 °C for KOH, to achieve sufficient vapour pressures in the cell. For KOH, reservoir temperatures between 600 and 750 °C result in vapour pressures in the range 5 – 130 Pa, which despite the lower cross section expected for KOH would provide sufficient absorption in the cell for reliable measurements. In contrast, NaOH vapour pressures are lower and temperatures around 900 °C would be required to achieve vapour pressures on the order of 30–50 Pa necessary to achieve sufficient absorption. Alternatively, improved sensitivity and detection at lower vapour pressures can be achieved by arranging dual passages through the cell increasing the absorption path length by a factor of two.

IV. CONCLUSIONS

The design and performance have been demonstrated for a calibration cell based on a cold finger, which can be employed to generate KCl vapour at stable well-defined concentration and temperature. The cell is suitable for UV absorption measurements to obtain calibration spectra or to perform detailed studies of the absorption cross section for KCl. Investigations using an instrument for UV absorption measurements of KCl showed that improved calibration and absolute accuracy for the instrument can be obtained compared with previous approaches. In addition, more reliable KCl UV absorption spectral profiles and cross sections have been measured over different chosen temperatures. The concept of the calibration cell can equally be employed for investigations of other alkali chlorides such as NaCl or hydroxides, i.e., KOH and NaOH. In other words, the cell has potential to be used for detailed spectroscopic studies of high relevance for development of

alkali-measuring devices used in biomass combustion to determine concentrations in the flue gas. This research has thus proven the working hypothesis in that the new design of the calibration cell is fit for this purpose.

SUPPLEMENTARY MATERIAL

See supplementary material for a description of how the coefficients A, B, and C in the Antoine equation were determined.

ACKNOWLEDGMENTS

The Swedish Energy Agency through the Centre for Combustion Science and Technology (CECOST), the Knut and Alice Wallenberg foundation, and Vattenfall AB are gratefully acknowledged for their financial support. Finally, Leif Lundberg and co-workers at Scientific Lab Glass AB in Lund are greatly acknowledged for their help in the construction and development of the furnace and calibration cell

[1]T. Leffler, C. Brackmann, M. Berg, Z. S. Li, and M. Aldén, Ind. Combust. J. Int. Flame Res. Found. 201601 (2016), available at http://www.industrial.combustion.ifrf.net/paper_download.html?paperId=134.
[2]C. S. Andersson, European patent EP 1354167 (2006).
[3]H. Kassman, J. Pettersson, B. M. Steenari, and L. E. Åmand, Fuel Process Technol. **105**, 170–180 (2013).
[4]P. Monkhouse, Prog. Energy Combust. Sci. **37**(2), 125–171 (2011).
[5]T. Sorvajärvi, N. DeMartini, J. Rossi, and J. Toivonen, Appl. Spectrosc. **68**(2), 179–184 (2014).
[6]T. Leffler, C. Brackmann, A. Ehn, B. Kaldvee, M. Aldén, M. Berg, and J. Bood, Appl. Opt. **54**(5), 1058–1064 (2015).
[7]C. S. Andersson, European patent EP 1221036 (2006).
[8]C. Forsberg, M. Broström, R. Backman, E. Edvardsson, S. Badiei, M. Berg, and H. Kassman, Rev Sci Instrum. **80**(2), 023104 (2009).
[9]A. Grosch, V. Beushausen, H. Wackerbarth, O. Thiele, and T. Berg, Appl. Opt. **49**(2), 196–203 (2010).
[10]P. Davidovits and D. C. Brodhead, J. Chem. Phys. **46**(8), 2968–2973 (1967).
[11]U. Platt and D. Perner, in *Optical and Laser Remote Sensing*, edited by D. K. Killinger and A. Mooradian (Springer-Verlag, Berlin, Heidelberg, New York, 1983), Vol. 39, pp. 97–105.
[12]W. J. M. Vanderkemp, L. C. Jacobs, H. A. J. Oonk, and A. Schuijff, J. Chem. Thermodyn. **23**(6), 593–604 (1991).
[13]G. W. Thomson, Chem. Rev. **38**(1), 1–39 (1946).
[14]A. Roine, *HSC Chemistry for Windows Version 7.1* (Outokumpu Research, Pori, Finland 2011).
[15]IVTAN Association, *Izhorskaya 13/19*, *127412 Moscow*, *Russia*, *1994*.
[16]Society of American Chemical, American Institute of Physics, and Society of National Bureau, *JANAF Thermochemical Tables: Part 1, Part 2* (The American Chemical Society and the American Institute of Physics for the National Bureau of Standards, 1985).
[17]D. G. Archer, J. Phys. Chem. Ref. Data **28**(1), 1–17 (1999).
[18]I. Barin, *Thermochemical Data of Pure Substances. Part I* (VCH, Weinheim, Federal Republic of Germany; New York, 1993).
[19]I. Barin, *Thermochemical Data of Pure Substances. Part II* (VCH, Weinheim, Federal Republic of Germany; New York, 1993).
[20]I. Barin, O. Knacke and O. Kubaschewski, *Thermochemical Properties of Inorganic Substances: Supplement* (Springer-Verlag, Berlin, New York, 1977).
[21]I. Barin, O. Kubaschewski, and O. Knacke, *Thermochemical Properties of Inorganic Substances* (Springer-Verlag, Berlin, 1973).
[22]I. Barin, E. Schultze-Rhonhof, W. S. Sheng, and F. Sauert, *Thermochemical Data of Pure Substances* (VCH, Weinheim, 1989).
[23]G. V. Belov, V. S. Iorish, and V. S. Yungman, Calphad **23**(2), 173–180 (1999).
[24]M. W. Chase and Society of American Chemical, *JANAF Thermochemical Tables: Part II, Cr-Zr* (American Chemical Society, Washington, 1985).
[25]M. W. Chase and Society of National Institute and Technology, *NIST-JANAF Thermochemical Tables* (American Chemical Society, American Institute of Physics for the National Institute of Standards and Technology, Washington, DC; Woodbury, NY, 1998).
[26]H. Landolt, R. Börnstein, and E. Scientific Group, *Thermodata* (Springer, Berlin, 1999).
[27]J. E. Mayer and I. H. Wintner, J. Chem. Phys. **6**(6), 301–306 (1938).
[28]C. M. Western, PGOPHER, a program for simulating rotational structure, version 7.1.108, University of Bristol, 2010, http://pgopher.chm.bris.ac.uk.
[29]E. J. Barton, C. Chiu, S. Golpayegani, S. N. Yurchenko, J. Tennyson, D. J. Frohman, and P. F. Bernath, Mon. Not. R. Astron. Soc. **442**(2), 1821–1829 (2014).
[30]B. L. Chadwick, G. Domazetis, and R. J. S. Morrison, Anal. Chem. **67**(4), 710–716 (1995).
[31]R. C. Oldenborg and S. L. Baughcum, Anal. Chem. **58**(7), 1430–1436 (1986).
[32]D. E. Self and J. M. C. Plane, Phys. Chem. Chem. Phys. **4**(1), 16–23 (2002).